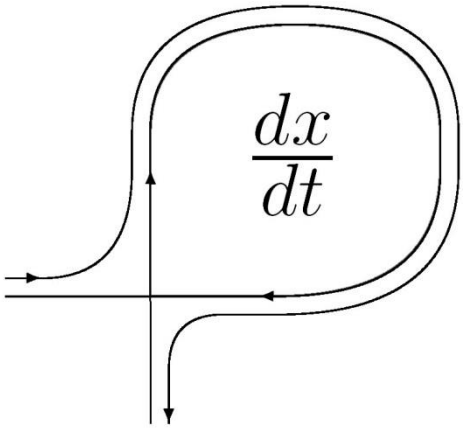

DIFFERENTIAL EQUATIONS
AND
CONTROL PROCESSES
N. 3, 2024
Electronic Journal,
reg. № ФС77-39410 at 15.04.2010
3ISSN 1817-2172

http://diffjournal.spbu.ru/
e-mail: jodiff@mail.ru

Differential equations with randomness;
filtration and identification;
numerical methods

Analysis of algorithms of numerical implementations for the Wonham filter under uncertainty in measurement noise covariance

Bosov A.V.[1,*], Kudryavtseva I.A.[2,**]

[1]Federal Research Center "Computer Science and Control" of the Russian Academy of Sciences;
[2]Moscow Aviation Institute (National Research University);
[*]abosov@ipiran.ru
[**]kudryavtseva.irina.a@gmail.com

Abstract. The paper addresses the filtering of a continuous-time Markov chain states that can be observed through linear measurements perturbed by a Wiener process. There is supposed the presence of uncertainty in the intensity of measurement noise. The problem is worked out under the assumption of unknown intensity but subject to its known upper bound. If there is no uncertainty in measurements the optimal solution is provided by the Wonham filter that doesn't ensure stable numerical implementations. The paper exposes that the Wonham filter shows robustness in the presence of uncertainty if model's parameters don't imply its divergent. It is detected that to cope with divergence tracking and handling trajectories aren't sufficient in the case of uncertainty. The more efficient way is to consider discretized approximations of the Wonham filter implemented for a discrete model that approximates the initial continuous-time measurement system. Such an approach perceptibly advantages if numerical implementations contain divergent trajectories. If there are no divergent trajectories, then the discretized filters give a slightly worse result but acceptable.

Keywords: filtering problem, nonlinear filtering, Wonham filter, minimax estimation, Markov chain.

1. Introduction

Filtering is one of the crucial problems in studying dynamical systems. Estimating random hidden process's states from noise-contaminated measurements represents the matter of the stochastic filtering problem. As is well known, in the case of linear models under assumption about Gaussian-distributed underlying processes the optimal solution can be obtained by the Kalman-Bucy filter while the Kushner-Stratonovich filter is employed for the exact same purpose when nonlinear models are considered [1-3].

In general, nonlinear filtering is challenging due to the lack of a finitely dimensional system of a sufficient amount of statistics for a posterior distribution. That implies to utilizing various finitely dimensional approximations [3-6].

The other complexity lies in appearing uncertainty in a model. Optimal filtering algorithms are highly sensitive to deviations from nominal settings and their efficient performance might degrade. By virtue of this developing robust state estimation strategies are of notable importance. There can be given several strategies as an illustration: the contemporary H_∞ filtering algorithm [7, 8], its combination with classical least square techniques (the mixed H_2/H_∞) [9], receding horizon estimation [10, 11], a robust filter based on a convex quadratic problem expressed in terms of LMI [12], the minimax approaches [13-17].

It is worth mentioning that there is a variety of interpretations for "robustness". Herein the considered robust algorithms can be treated in terms of stability of estimates with respect to existing uncertainty.

In the paper, the system uncertainty related to a lack of a prior information about measurement noise intensities is devoted attention to. The minimax approach is taken for construction a robust filter. The idea behind the minimax approach is that the filtering problem is being solved provided that the worst scenario from some uncertainty set containing values and statistics of undefined parameters is implemented [16, 17].

Nonlinear filtering for a continuous-time Markov chain with finite state space is considered. In other words, the Wonham filtering problem is being solved [18, 19]. It should be kept in mind that the Wonham filter is essentially nonlinear and its straightforward solution doesn't seem possible to obtain. However, in practice it is more relevant to focus on robustness of numerical approximations for the Wonham filter. This is the topic of further discussion in the current work.

The remainder of this paper is organized as follows. The filtering problem is formulated in Sect. 1. The optimal solution for the problem with no uncertainty and its robust approximation schemes are given in Sect. 2. Sect. 3 reveals a huge amount of numerical experiments for a vast range of parameters values to perform comparative analysis where the discretized filters are involved for the purpose. The paper is summarized in Sect. 4.

2. Problem Formulation

Let $(\Omega, \mathcal{F}, \mathcal{P}, \mathcal{F}_t)$, $t \in [0, T]$, be a probability space equipped with a filtration. Suppose that the stochastic system whose states evolution is described by means of the equation defining a Markov jump process, a Markov chain with the state space produced by a set of unit coordinate vectors $\{e_1, \dots, e_n\}$, $e_j \in \mathbb{R}^{n_y}$, $j = 1, \dots, n$:

$$dy_t = \Lambda_t' y_t dt + d\Lambda_t^y, \quad y_0 = Y, \tag{1}$$

is observed through linear measurements satisfying the equation:

$$dz_t = a_t y_t dt + b_t z_t dt + \sigma_t dw_t, \quad z_0 = Z, \tag{2}$$

where $y_t \in \mathbb{R}^{n_y}$ is the system state vector, $z_t \in \mathbb{R}^{n_z}$ is the measurement vector, Λ_t is the transition intensity matrix of the Markov chain governed by equation (1), Λ_t' is the transpose of Λ_t, Λ_t^y is the $\mathcal{F}_t$-martingale, the vector $Y \in \mathbb{R}^{n_y}$ is the initial vector having the known probability distribution π_0, the vector $Z \in \mathbb{R}^{n_z}$ is a Gaussian random vector with known characteristics $\mathcal{E}\{Z\}, \mathcal{E}\{ZZ'\}$, $w_t \in \mathbb{R}^{n_w}$ is the standard Wiener process independent of Λ_t^y, Y, Z, $\mathcal{F}_t^z$ is the σ -algebra generated by measurements presented by equation

(2), meanwhile $\mathcal{F}_t^z \subseteq \mathcal{F}_t \subseteq \mathcal{F}$, the matrix functions $a_t \in \mathbb{R}^{n_z \times n_y}$, $b_t \in \mathbb{R}^{n_z \times n_z}$, $\sigma_t \in \mathbb{R}^{n_z \times n_w}$ are presumed to be bounded:

$$|a_t| + |b_t| + |\sigma_t| \leq C \quad \forall t \in [0, T],$$

that guaranties the existence of a solution of equation (2). Moreover, measurement errors are non-degenerative, namely $\sigma_t \sigma_t{}' > 0$. The notation $|\cdot|$ stands for a matrix norm. The symbols $\mathcal{E}\{\cdot \mid \cdot\}, \mathcal{E}\{\cdot\}$ mean a conditional and unconditional expectations respectively.

The presented problem is considered under assumption of the lack of information about exact values of measurement errors intensity given by $\sigma_t \sigma_t{}' \leq \Sigma_t$ but under conditions of knowing the upper bound of the noise covariance $\Sigma_t > 0$. The matrix inequality $K \leq K'$ should be interpreted as $K - K' = K'' \leq 0$ where K'' is a positive semidefinite matrix. The goal of the paper is to examine quality of the algorithms to estimate the chain state y_t through measurements subject to the claimed above restriction.

The exact filtering problem solution expressed as

$$\hat{y}_t^{minmax} = \arg\min_{\hat{y}_t} \max_{\sigma_t : \sigma_t \sigma_t' \leq \Sigma_t} \mathcal{E}\{|\hat{y}_t - y_t|^2\}$$

is tough to obtain, however, it can be done if supposing that

$$\hat{y}_t^{minmax} \approx \hat{y}_t^W(\Sigma_t), \hat{y}_t^W(\sigma_t \sigma_t') = \mathcal{E}\{y_t | \mathcal{F}_t^z, \sigma_t\}.$$

The latter should be treated as the optimal Wonham filter without uncertainty if the covariance $\sigma_t \sigma_t{}'$ was given but in fact replaced with the upper bound Σ_t. In the problem without uncertainty the optimal solution can be defined as [18, 19]:

$$d\hat{y}_t^W = \Lambda_t' \hat{y}_t^W dt + (\mathrm{diag}(\hat{y}_t^W) - \hat{y}_t^W (\hat{y}_t^W)') a_t{}' \Sigma_t^{-1} (dz_t - a_t \hat{y}_t^W dt - b_t z_t dt). \quad (3)$$

Unfortunately, such an approach does not permit to obtain the desired estimate of the state y_t in practice because when switching into numerical implementation of the optimal Wonham filter (3) by using the Euler-Maruyama scheme the stability of computational procedure fails (a sequence of approximations is divergent) [20, 21]. Consequently, finding stable algorithms but actually not optimal is more worth.

The paper accentuates on the case when the measurement noise intensity is unknown. The Wonham filter and the discretized filters described in detail in [22, 23] are considered as the baseline algorithms. In the paper for each of the filters the unknown intensity is replaced with the upper bound Σ_t. It should be underlined that analytical examination for the algorithms accuracy and the comparative study cannot be done. Additionally, it is worth noting that evolution of the filters trajectories is affected by as far as robust the algorithms are. That, in turn, depends on the parameters in the measurement equation.

Thus, the goal of the paper is to propose the computational model that has a value in practice and to carry out a series of numerical experiments under various initial conditions varying the parameters of the model, changing values of the upper bound Σ_t. A wide range of the model variations can be obtained in such a way. That permits to carry out extensive modelling to identify specificities of behavior of the filters and to assess the accuracy.

3. Discretized Representations of the Wonham Filter

Discretizing equations (1) and (2) over time interval $[0, T]$ with a given fixed time step δ:

$$t_0 = 0,\ t_i = t_0 + i \cdot \delta, i = 1, \dots, \left[\frac{T}{\delta}\right],$$

([.] means the floor function) leads to stable approximations of the Wonham filter, that is shown in [22].

In addition to that the matrices a_t, b_t, σ_t are assumed to be constant on subintervals $[t_{i-1}, t_i]$. This can be accomplished by swapping them for piecewise constant approximations.

For further explanation the process z_t^0 being the anticipating transformation of z_t should be introduced [22]:

$$z_t^0 = \int_0^t (dz_\tau - b_\tau z_\tau)d\tau = \int_0^t (a_\tau y_\tau d\tau + \sigma_\tau dw_\tau). \tag{4}$$

It holds due to the fact that

$$\hat{y}_t = \mathcal{E}\{y_t|\mathcal{F}_t^z\} = \mathcal{E}\{y_t|\mathcal{F}_t^{z^0}\}$$

is met.

Consider new measurements $\Delta z_{t_i}^0$ discretized in time with step δ:

$$\Delta z_{t_i}^0 = \int_{t_{i-1}}^{t_i} (a_\tau y_\tau d\tau + \sigma_\tau dw_\tau).$$

The increments $\Delta z_{t_i}^0$ generate the σ -algebra $\mathcal{F}_t^{\Delta z^0} = \sigma\left\{\Delta z_{t_j}^0, j = 1, .., i\right\}$. Then, the estimate $\hat{y}_t = \mathcal{E}\{y_t|\mathcal{F}_t^{\Delta z^0}\}$ can be defined via the following recurrent formula [23]:

$$\begin{aligned}
&\hat{y}_{t_i}^{opt} = \left(\mathbf{1}\hat{q}_{t_i}'\hat{y}_{t_{i-1}}^{opt}\right)^{-1}\left(\hat{q}_{t_i}'\hat{y}_{t_{i-1}}^{opt}\right),\\
&\hat{q}_{t_i}^{k,j} = \mathcal{E}\left\{\mathcal{N}\left(\Delta z_{t_i}^0; a\mu_i, \delta\sigma\sigma'\right)y_{t_i}^j \,\middle|\, y_{t_{i-1}} = e_k\right\},\\
&\hat{y}_{t_i}^{opt} = \pi_0,
\end{aligned} \tag{5}$$

where $\mu_i = \int_{t_{i-1}}^{t_i} y_\tau d\tau = \left(\mu_i^1, \dots, \mu_i^{n_y}\right)$ is taken for a random vector whose components are equal to time the Markov chain stays in each possible state on the interval $(t_{i-1}, t_i]$,

$$\mathcal{N}(z; m, \sigma\sigma') = \frac{1}{\sqrt{\det(\sigma\sigma')(2\pi)^{n_z}}} \exp\left\{-\frac{1}{2}(z-m)'(\sigma\sigma')^{-1}(z-m)\right\}$$

is the multivariate Gaussian probability distribution with the mean m and covariance matrix $\sigma\sigma'$, $\mathbf{1} = (1, \dots, 1)' \in \mathbb{R}^{n_y}$ is a vector of ones, $a_t = a = \text{const},\ \sigma_t = \sigma = \text{const}$. The entries $\hat{q}_{t_i}^{k,j}$ of the matrix $\hat{q}_{t_i} = \left\{\hat{q}_{t_i}^{k,j}\right\}_{k,j=1}^{n_y}$ can be calculated by applying numerical approximations in accordance with the different schemes [23]: the left-point rule; the middle point rule; the Gauss quadrature schemes.

The left-point rule will hereinafter be used as a base formula in calculation since the estimates obtained by the rest two mentioned rules have demonstrated absolutely identical properties that is shown in [23]. The left-point rule provides the estimate $\breve{y}_{t_i}^{\delta\frac{1}{2}}$ with an error of order $1/2$.

It should be additionally noticed that the essence of the transformation (4) lies in treating the matrix coefficient b_t as 0 in (2). That incidentally holds true for both discretized filters and the Wonham filter. However, this is the coefficient that tremendously affects the stability of numerical process for the Wonham filter.

4. Numerical experiments

4.1. Model description

The claimed analysis has been carrying out by treating the model of a mechanic actuator as an element of an overhead crane system [23]. Suppose, the actuator causes movement of a trolley along a rail. The trolley should be positioned at several fixed locations on the rail (states). Let x_t and v_t be an actuator state and its velocity respectively. The velocity is determined by a force linearly depending on the state x_t and the velocity v_t and also a vector y_t serving to describe required positions of the trolley. From the physical point of view the problem lies in stabilizing the actuator at states defined by $y_t = e_i$ being states of the Markov chain. The system can be represented in the form [23]:

$$\begin{aligned} dx_t &= v_t dt, \qquad t \in (0,T], \\ dv_t &= ax_t dt + bv_t dt + cy_t dt + \sqrt{g} dw_t, \end{aligned} \tag{6}$$

where the constants a, b, g and the vector c are known, w_t is the standard Wiener process, y_t is an unobservable process subject to be estimated through (x_t, v_t) as measurements. The process y_t is supposed to be a three- or four-state Markov jump process: $n_y = 3$ or $n_y = 4$. The transition intensity matrix $\Lambda_t = = \Lambda = const$:

$$\Lambda = \begin{pmatrix} -0.5 & 0.5 & 0 \\ 0.5 & -1 & 0.5 \\ 0 & 0.5 & -0.5 \end{pmatrix} \text{ or } \Lambda = \begin{pmatrix} -5 & 5 & 0 \\ 5 & -1 & 5 \\ 0 & 5 & -5 \end{pmatrix}$$

for $n_y = 3$ and

$$\Lambda = \begin{pmatrix} -0.5 & 0.5 & 0 & 0 \\ 0.5 & -1 & 0.5 & 0 \\ 0 & 0.5 & -1 & 0.5 \\ 0 & 0 & 0.5 & -0.5 \end{pmatrix} \text{ or } \Lambda = \begin{pmatrix} -5 & 5 & 0 & 0 \\ 5 & -10 & 5 & 0 \\ 0 & 5 & -10 & 5 \\ 0 & 0 & 5 & -5 \end{pmatrix}$$

for $n_y = 4$.

The initial state $y_0 = Y = e_1$ is specified by the probability distribution $\pi_0 = (1,0,0)'$ or $\pi_0 = (1,0,0,0)'$ depending on dimensionality. x_0, v_0 are supposed to be independent Gaussian variables with the zero mean and the variances $\sigma_x = 1, \sigma_v = 1$. Moreover, a note should be made regarding y_t is that y_t is a homogeneous Markov process with the limiting distribution

$$\pi_\infty = \left(\frac{1}{3}, \frac{1}{3}, \frac{1}{3}\right)'$$

for $n_y = 3$ and

$$\pi_\infty = \left(\frac{1}{4}, \frac{1}{4}, \frac{1}{4}, \frac{1}{4}\right)'$$

for $n_y = 4$.

The coefficients a, b are varied in calculation while the vector c is set to be

$$c = (c_1, c_2, c_3) = (-1, 0, 1) \text{ or } c = (c_1, c_2, c_3) = (1, 2, 4)$$

if $n_y = 3$ and

$$c = (c_1, c_2, c_3, c_4) = (-1.5, -0.5, 0.5, 1.5)$$

if $n_y = 4$.

Varying the parameters listed above one can change such qualitative characteristics of system (6) as transition intensities (low/high), state space dimension (lower-dimensional state space / higher-dimensional state space), states of the Markov chain (symmetric with respect to the origin / biased with respect to the origin). Besides that, different values of the coefficients a, b in (6) are considered to produce stable and unstable systems.

It is worth mentioning that system (6) is stable if $b < 0$ and $b^2 + 4a < 0$ as $\frac{b \pm \sqrt{b^2+4a}}{2}$ are eigenvalues of the system matrix

$$b_t = \begin{pmatrix} 0 & 1 \\ a & b \end{pmatrix}$$

and unstable otherwise. Therefore, the coefficients a, b are assigned to both negative and positive values in numerical experiments (see Section 4.2).

The Euler-Maruyama method is applied to perform integration in all cases for both system (6) and filter models (3) and (5) with step $\delta = 10^{-3}$. A discrete time Markov chain approximating y_t is being simulated by independent exponentially distributed random variables if taking 100 intervals for each integration interval of length δ, namely sampling is produced from $E(0.00001)$ distribution. The integration step for observation system (6) is similarly divided into 100 intervals of length $\frac{\delta}{100}$.

As it is mentioned and perfectly illustrated in [23] the Euler-Maruyama scheme leads to divergence of some trajectories' estimates because of its instability. According to the presented results in [23] mostly for every trajectory there are points where the nonnegativity property or normalization or even both are not met. To diminish the impact caused by failure of the aforementioned conditions simple adjustments have been done.

If the condition $|(\hat{y}_\tau^W)_k| > 1$ is hold for at least one k then there presents the divergence. Two techniques can be offered to avert divergence. According to the first one, in the case of satisfaction of $|(\hat{y}_\tau^W)_k| > 1$ the estimate turns back to the limit state $\hat{y}_\tau^W = \pi_\infty$ at the moment τ when the divergence test gets gratified. The estimate modified in such a way is denoted as $\hat{y}_t^{lim}$ where the superscript indicates the involvement of the limit state π_∞. Following the second one, the estimate $\hat{y}_\tau^W$ at the considered moment gets replaced with the estimate $\hat{y}_{\tau-\delta}^W$ received at the previous step. That gives the estimate $\hat{y}_t^{del}$ where the superscript underlines its "delay" nature. These are two sorts of estimates that will be examined for robustness later and these are the estimates which attention is paid to as a goal of the paper.

To assess the quality of estimation of the aforementioned $\hat{y}_t^{lim}$, $\hat{y}_t^{del}$, $\breve{y}_{t_i}^{\delta^{\frac{1}{2}}}$ the mean square error are calculated from obtained 1000 trajectories and filter estimates:

$$\widehat{\mathcal{D}}(\hat{y}_t^{lim}), \widehat{\mathcal{D}}(\hat{y}_t^{del}), \widehat{\mathcal{D}}\left(\breve{y}_{t_i}^{\delta^{\frac{1}{2}}}\right) \text{ calculated as } \widehat{\mathcal{D}}(\tilde{y}_{t_i}) = \hat{\mathcal{E}}\left\{\frac{\delta}{T}\sum_{i=1}^{\frac{T}{\delta}}(cy_{t_i} - c\tilde{y}_{t_i})^2\right\},$$

where $\hat{\mathcal{E}}$ means averaging over 1000 trajectories.

To investigate for robustness with respect to the unknown measurement errors intensity numerical computations are performed for the chosen noise intensity $\sqrt{g} = 0.1$ but under the assumption of solely known Σ_t. Three options for Σ_t are considered:

- $\Sigma_t = g$ (the problem with complete information about parameters of the noise);
- $\Sigma_t = 3g$ (the upper bound of the intensity is "close" to its true value);
- $\Sigma_t = 10g$ (the upper bound of the intensity is "far" from its true value).

In addition to that calculations are supplemented by considering two more cases when g is known and it is three and ten times the initially chosen value.

4.2. Stable system

In the paper, two scenarios regarding principally distinct behavior of the system (with stable and unstable measurements) are analyzed. The situation when the parameters $a = -1, b = -0.5$ comes within the stable measurements case and is treated as an illustrative example of that scenario. For the unstable measurements it is supposed that $a = 1, b = 0.5$. Moreover, as claimed earlier the parameter b can be formally nullified, however, it turns out that the case when $a = 0, b = 0$ can play a significant role for numerical filter's implementations. That is the reason to single that case out in particular.

Computations are organized as follows. At first the stable measurements are focused on. In Section 4.3 the unstable measurements will be paid attention to. Series of computational experiments are separately conducted for each of the cases with different given values of the parameters n_y, Λ, c. Along with computations executed for $g = 0.01$ and $\Sigma_t = g, 3g, 10g$ each series of experiments are complemented by the situations for $g = 0.01 \times 3 = 0.03, g = 0.01 \times 10 = 0.1$ to compare. The tables below present the results for each considered series of the experiments. The tables are preceded by a list of the corresponding parameters.

The first series of computations replicates the scenario in [23] and is given in Tab. 1.

Tab. 1. Experiment results. Stable system

$a = -1, b = -0.5, n_y = 3, (c_1, c_2, c_3) = (-1, 0, 1), \Lambda = \begin{pmatrix} -0.5 & 0.5 & 0 \\ 0.5 & -1 & 0.5 \\ 0 & 0.5 & -0.5 \end{pmatrix}$, $a = 0, b = 0$ (for elaborate explanation see section 4.3)			
g, Σ_t	$\widehat{\mathcal{D}}(\hat{y}_t^{lim})$	$\widehat{\mathcal{D}}(\hat{y}_t^{del})$	$\widehat{\mathcal{D}}\left(\breve{y}_t^{\delta^{\frac{1}{2}}}\right)$
$g = 0.01, \Sigma_t = 0.01$	0.0540	0.0495	0.0486
$\boldsymbol{g = 0.01, \Sigma_t = 0.03}$	**0.0612**	**0.0612**	*0.0729*
$\boldsymbol{g = 0.01, \Sigma_t = 0.1}$	**0.0911**	**0.0911**	0.1225
$g = 0.03, \Sigma_t = 0.03$	0.0987	0.0987	*0.0986*
$g = 0.1, \Sigma_t = 0.1$	0.1837	0.1837	0.1837

Hereinafter the rows corresponding to computations with uncertainty (for $\Sigma_t = 3g$, $\Sigma_t = 10g$) are highlighted in bold, the accuracy of the estimates of the discretized filters for the model with uncertainty and for the corresponding model with the intensity $3g$ are placed in light-grey cells and the accuracy of the

discretized filters for the model with uncertainty $\Sigma_t = 10g$ and for the corresponding model with the intensity $10g$ are situated in dark-grey cells. Highlighting cells in the tables makes the comparison of the accuracy for the model with uncertainty and for the worst case easier. The bold values correspond to the results for the models with uncertainty and they are the ones that are used to analyze the robustness.

According to Tab. 1, the results agree with earlier ones obtained in [23]. It must be pointed out that when trajectories contain points with violation of the condition (it corresponds to the first row) the discretized filters demonstrate better quality than the heuristic estimates. However, this property breaks for further cases when the filter approximations $\hat{y}_t^{lim}$, $\hat{y}_t^{del}$ get preferable. In two last experiments there are not trajectories with divergence and all the filters show up approximately close results. The discretized filters can be still claimed to provide robustness nevertheless.

The tables are accompanied by graphical illustrations. The graphs demonstrate results obtained in one chosen experiment for each model. The figures present distinctive state trajectories, trajectories of the filters estimates and dynamics of $\hat{d}_{t_i}(\tilde{y}_{t_i}) = \hat{\mathcal{E}}\left\{\left(cy_{t_i} - c\tilde{y}_{t_i}\right)^2\right\}$ involved in obtaining the integral square estimates of the filters' accuracy $\widehat{\mathcal{D}}(\hat{y}_t^{lim})$, $\widehat{\mathcal{D}}(\hat{y}_t^{del})$, $\widehat{\mathcal{D}}\left(\breve{y}_{t_i}^{\delta^{\frac{1}{2}}}\right)$. The listed above results for the first case are given in Fig. 1.

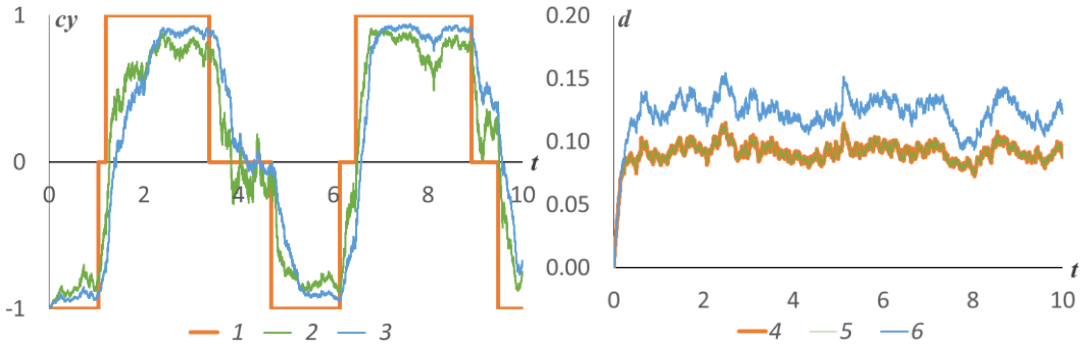

a) b)

Fig. 1. Model 1, scenario 3: $g = 0.01, \Sigma_t = 0.1$

a) 1 – cy_t, 2 – $c\hat{y}_t^{lim}$ ($c\hat{y}_t^{del}$is identical), 3 – $\breve{y}_{t_i}^{\delta^{\frac{1}{2}}}$

b) 4 – $\hat{d}_t(\hat{y}_t^{lim})$, 5 – $\hat{d}_t(\hat{y}_t^{del})$, 6 – $\hat{d}_t\left(\breve{y}_{t_i}^{\delta^{\frac{1}{2}}}\right)$

For further analysis let's make the actuator's running more complicated by significantly increasing intensities. It can be done by getting entries of the transition intensity matrix Λ_t larger. Tab. 2 exposes experiment results. Fig. 2 supplies the case with corresponding graphs.

Tab. 2. Experiment results. Stable system.
The case of lager intensities

$a = -1, b = -0.5, n_y = 3, (c_1, c_2, c_3) = (-1, 0, 1), \Lambda = \begin{pmatrix} -5 & 5 & 0 \\ 5 & -1 & 5 \\ 0 & 5 & -5 \end{pmatrix}$, $a = 0, b = 0$ (for elaborate explanation see section 4.3)			
g, Σ_t	$\widehat{\mathcal{D}}(\hat{y}_t^{lim})$	$\widehat{\mathcal{D}}(\hat{y}_t^{del})$	$\widehat{\mathcal{D}}\left(\breve{y}_t^{\delta^{\frac{1}{2}}}\right)$
$g = 0.01, \Sigma_t = 0.01$	0.1959	0.1956	0.1948
$\boldsymbol{g = 0.01, \Sigma_t = 0.03}$	**0.2164**	**0.2164**	*0.2286*
$\boldsymbol{g = 0.01, \Sigma_t = 0.1}$	**0.3247**	**0.3247**	0.3250
$g = 0.03, \Sigma_t = 0.03$	0.3055	0.3055	*0.3064*
$g = 0.1, \Sigma_t = 0.1$	0.4477	0.4477	0.4485

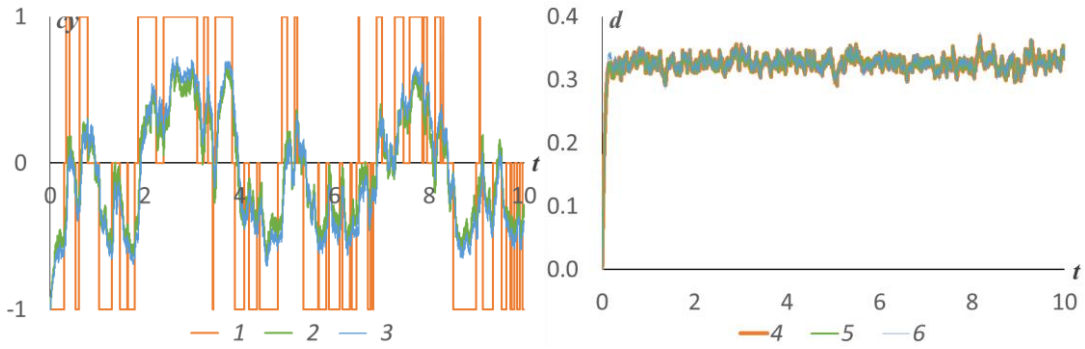

Fig. 2. Model 2, scenario 3: $g = 0.01, \Sigma_t = 0.1$

a) $1 - cy_t$, $2 - c\hat{y}_t^{lim}$ ($c\hat{y}_t^{del}$is identical), $3 - \breve{y}_{t_i}^{\delta\frac{1}{2}}$

b) $4 - \hat{d}_t(\hat{y}_t^{lim})$, $5 - \hat{d}_t(\hat{y}_t^{del})$, $6 - \hat{d}_t\left(\breve{y}_{t_i}^{\delta\frac{1}{2}}\right)$

The results reveal the same particularity of numerical implementation of the discretized filters. Although more closeness is traced in results. The filter's approximations faintly leave behind the discretized filters in quality of estimates. Moreover, in spite of increasing transition intensity a number of cases when the divergence test has been satisfied hasn't grown in comparison with the previous series of experiments. Both the discretized filters and the filter's approximations showcase robustness with respect to uncertainty.

In the next series of experiments higher-dimensional state space is considered that implies the increase in the complexity of the Wonham filter implementations.

The results presented in Tab. 3 really exemplify the scenario when the discretized filters have the edge over the Wonham filter approximations. That is clearly seen if focusing on the middle values of the last column in Tab. 3. The results in Tab. 3 are also supplemented with the graphs in Fig. 3.

Tab. 3. Experiment results. Stable system.
The higher-dimensional state space case

$a = -1, b = -0.5, n_y = 4, = (-1.5, -0.5, 0.5, 1.5), \Lambda = \begin{pmatrix} -0.5 & 0.5 & 0 & 0 \\ 0.5 & -1 & 0.5 & 0 \\ 0 & 0.5 & -1 & 0.5 \\ 0 & 0 & 0.5 & -0.5 \end{pmatrix}$, $a = 0, b = 0$ (for elaborate explanation see section 4.3)			
g, Σ_t	$\widehat{\mathcal{D}}(\hat{y}_t^{lim})$	$\widehat{\mathcal{D}}(\hat{y}_t^{del})$	$\widehat{\mathcal{D}}\left(\breve{y}_t^{\delta\frac{1}{2}}\right)$
$g = 0.01, \Sigma_t = 0.01$	0.3615	0.3562	0.0534
$\boldsymbol{g = 0.01, \Sigma_t = 0.03}$	**0.3583**	**0.3583**	*0.0811*
$\boldsymbol{g = 0.01, \Sigma_t = 0.1}$	**0.3751**	**0.3751**	0.1384
$g = 0.03, \Sigma_t = 0.03$	0.3957	0.3957	*0.1086*
$g = 0.1, \Sigma_t = 0.1$	0.4767	0.4767	0.2058

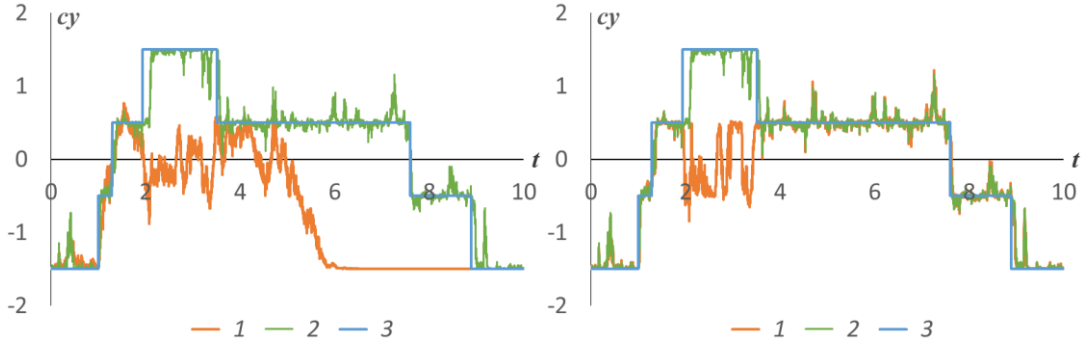

a) b)

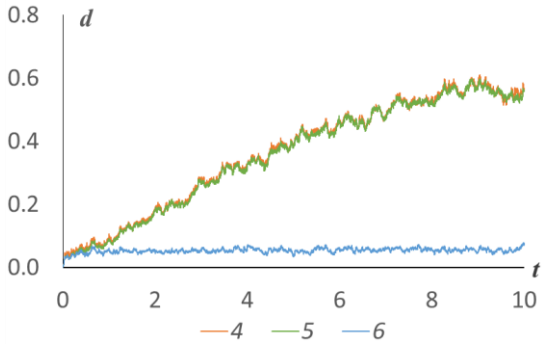

c)

Fig. 3. Model 3, scenario 1: $g = 0.01, \Sigma_t = 0.01$

a,b) 1 – cy_t, 2 – $c\hat{y}_t^{lim}$ ($c\hat{y}_t^{del}$is identical), 3 – $\breve{y}_{t_i}^{\delta^{\frac{1}{2}}}$

c) 4 – $\hat{d}_t(\hat{y}_t^{lim})$, 5 – $\hat{d}_t(\hat{y}_t^{del})$, 6 – $\hat{d}_t\left(\breve{y}_{t_i}^{\delta^{\frac{1}{2}}}\right)$

This is the main difference of the current scenario from the others, the fulfilment of the condition is not one-off and becomes regular that leads to dynamics shown in Fig. 3.

The filters approximations show up quit similar behavior that proves the same values of the accuracy. However, it is not an regularity establishing in time that will be seen later. What is more, the uncertainty in the model refines estimation quality in the sense of robustness.

All the filters showcase the robustness but advantages of the discretized filters are undoubted. It should be also added that the estimate of the accuracy given in Tab. 3 is increasing over time as the variances $\hat{d}_t(\hat{y}_t^{lim})$ and $\hat{d}_t(\hat{y}_t^{del})$ get larger. Unlike the listed variances the variance $\hat{d}_t\left(\breve{y}_{t_i}^{\delta^{\frac{1}{2}}}\right)$ remains constant. For the considered model the accuracy of the trivial estimate $\mathcal{E}\{y_t\}$ defined by its second moment in the steady state mode $\mathcal{E}\{|y_\infty|^2\} = \frac{2}{3}$. So, the estimates of the approximations are still informative.

Keeping values of the parameters unchanged except the intensity that is now 10 times the previous one a new series of experiments is launched. Tab. 4 displays the result while Fig. 4 demonstrates specific behavior. The accuracy of the trivial estimate $\mathcal{E}\{|y_\infty|^2\} = 1.25$ that points out informativity of the approximations.

Tab. 4. Experiment results. Stable system.
The higher-dimensional state space case with larger intensities

$a = -1, b = -0.5, n_y = 4, = (-1.5, -0.5, 0.5, 1.5), \Lambda = \begin{pmatrix} -5 & 5 & 0 & 0 \\ 5 & -1 & 5 & 0 \\ 0 & 5 & -1 & 5 \\ 0 & 0 & 5 & 5 \end{pmatrix}$, $a = 0, b = 0$ (for elaborate explanation see section 4.3)			
g, Σ_t	$\widehat{\mathcal{D}}(\hat{y}_t^{lim})$	$\widehat{\mathcal{D}}(\hat{y}_t^{del})$	$\widehat{\mathcal{D}}\left(\breve{y}_t^{\delta^{\frac{1}{2}}}\right)$
$g = 0.01, \Sigma_t = 0.01$	0.7073	0.7092	0.2247
$\boldsymbol{g = 0.01, \Sigma_t = 0.03}$	**0.7030**	**0.7030**	*0.2665*
$\boldsymbol{g = 0.01, \Sigma_t = 0.1}$	**0.7317**	**0.7317**	0.3869
$g = 0.03, \Sigma_t = 0.03$	0.8215	0.8216	*0.3668*
$g = 0.1, \Sigma_t = 0.1$	0.9820	0.9820	0.5852

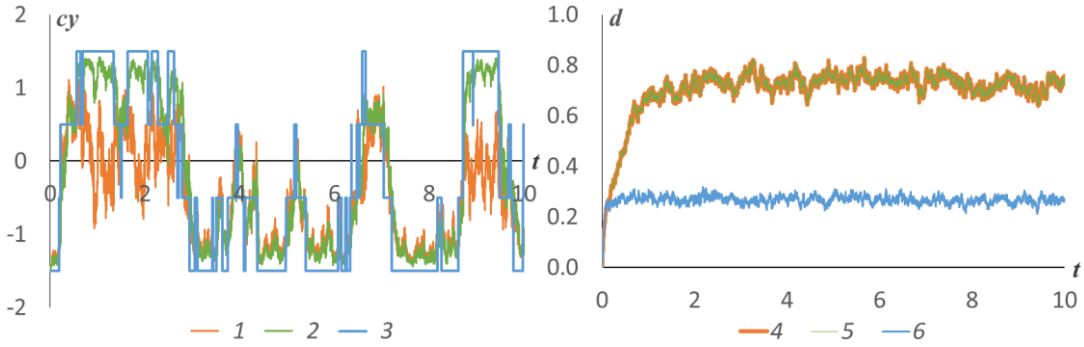

a) b)

Fig. 4. Model 4, scenario 2: $g = 0.01, \Sigma_t = 0.03$

a) 1 – cy_t, 2 – $c\hat{y}_t^{lim}$ ($c\hat{y}_t^{del}$is identical), 3 – $\breve{y}_{t_i}^{\delta^{\frac{1}{2}}}$

b) 4 – $\hat{d}_t(\hat{y}_t^{lim})$, 5 – $\hat{d}_t(\hat{y}_t^{del})$, 6 – $\hat{d}_t\left(\breve{y}_{t_i}^{\delta^{\frac{1}{2}}}\right)$

Increasing the intensity does not contribute to qualitative conclusions made for the previous model. Though the accuracy of all the filters equally reduces the filters are still robust. The discretized filters gain remarkably. The Wonham filter approximations are acceptable.

The last left out examination that is required to discuss is to violate symmetry of the chain. The obtained results are given in Tab. 5. Fig. 5 assists the results graphically. This series of experiments is supposed to be carried out under the same conditions as the first one (see Tab. 1)

Tab. 5. Experiment results. Stable system.
The asymmetric case

$a = -1, b = -0.5, n_y = 3, c = (1,2,4), \Lambda = \begin{pmatrix} -0.5 & 0.5 & 0 \\ 0.5 & -1 & 0.5 \\ 0 & 0.5 & -0.5 \end{pmatrix}$, $a = 0, b = 0$ (for elaborate explanation see section 4.3)			
g, Σ_t	$\widehat{\mathcal{D}}(\hat{y}_t^{lim})$	$\widehat{\mathcal{D}}(\hat{y}_t^{del})$	$\widehat{\mathcal{D}}\left(\breve{y}_t^{\delta^{\frac{1}{2}}}\right)$
$g = 0.01, \Sigma_t = 0.01$	0.2464	0.1255	0.0574
$\boldsymbol{g = 0.01, \Sigma_t = 0.03}$	**0.0752**	**0.0753**	*0.0945*
$\boldsymbol{g = 0.01, \Sigma_t = 0.1}$	**0.1153**	**0.1153**	0.1799
$g = 0.03, \Sigma_t = 0.03$	0.1448	0.1262	*0.1236*
$g = 0.1, \Sigma_t = 0.1$	0.2554	0.2554	**0.2548**

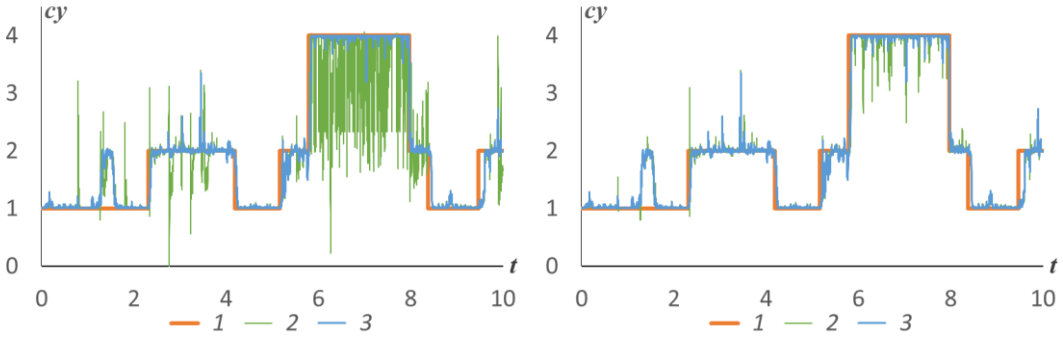

a) b)

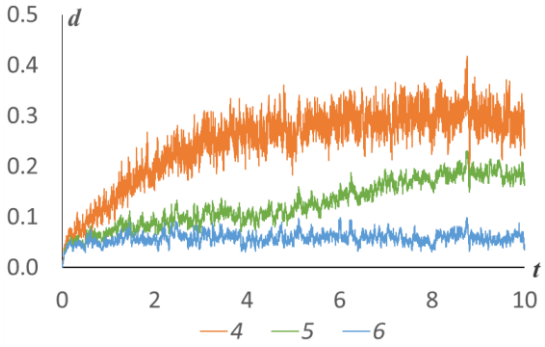

c)

Fig. 5. Model 5, scenario 1: $g = 0.01, \Sigma_t = 0.01$

a,b) 1 – cy_t, 2 – $c\hat{y}_t^{lim}$ ($c\hat{y}_t^{del}$), 3 – $\breve{y}_{t_i}^{\delta^{\frac{1}{2}}}$

c) 4 – $\hat{d}_t(\hat{y}_t^{lim})$, 5 – $\hat{d}_t(\hat{y}_t^{del})$, 6 – $\hat{d}_t\left(\breve{y}_{t_i}^{\delta^{\frac{1}{2}}}\right)$

The findings seemed absolutely unexpected. First of all, the approximations $\hat{y}_t^{lim}$ and $\hat{y}_t^{del}$ concede the estimate $\breve{y}_t^{\delta^{\frac{1}{2}}}$. A little benefit from this poor appearance of the approximations is that the utility of the estimates of the approximations is interpreted in such a sense that their accuracy is much better than the trivial estimate because $\mathcal{E}\{|y_\infty - \mathcal{E}\{y_\infty\}|^2\} = \frac{14}{9}$. However, the situation changes for the models with uncertainty and higher intensity. Moreover, the robustness of the approximations are more notable if comparing with the discretized filters. The filters get alike in behavior as the noise intensity is increasing. This example reveal that an numerical scheme of the Wonham filter that is initially unstable might be stable in the problem with uncertainty and exceed the discretized filters as a robust algorithm.

In summary, it can be stated that to predict behavior of the Wonham filter approximations cannot be done. Losses caused by instability of numerical computations can unexpectedly appear and influence the filtering quality. If parameters of a model are successfully chosen the approximations can take advantages and be more robust in behavior. The discretized filters always perform even under uncertainty as well but do not provide the desired reference solution when it becomes optimal.

4.2. Unstable system

It should be noted that system (6) gets actually unstable even if $a = 0, b = 0$. The system with values of the parameters leading to such a result can be called the system on the stability boundary. In fact, behavior of such a system turned out quite inert and there cannot be detected trajectories that diverge over $T = 10$. Repeated runs of the series of experiments given in Tab. 1-5 prove the statement above. In other words, the values $a = -1, b = -0.5$ can be replaced with $a = 0, b = 0$ leaving all other parameters unchanged. This gives the same results and permits not to change the content of the tables and the conclusions as consequence. This is the remark that is added in the headings of Tab. 1-5.

Switching to the unstable measurements case, suppose that $a = 1, b = 0.5$. One might assume that the situation will replicate the stability boundary case when $a = 0, b = 0$. But this is not the case. It is the instability of the measurements system itself that sufficiently influence numerical implementations. This fact is confirmed by the further set of experimental series. The first scenario is the model whose parameters coincide with the parameters from the first model except a, b ($a = 1, b = 0.5$).

The results are displayed in Tab. 6. The things that deserve special attention are the following. The discretized filters keep demonstrating the same advantage in estimation while the approximations are out of sense. Indeed, in the considered case the steady-state value $\mathcal{E}\{|y_\infty|^2\} = \frac{2}{3}$. It signifies that the trivial estimate $\mathcal{E}\{y_t\} = 0$ gets better in comparison with the approximations. Below Fig. 6 demonstrates specific behavior of the filters.

Tab. 6. Experiment results. Unstable system

$a = 1, b = 0.5, n_y = 3, (c_1, c_2, c_3) = (-1, 0, 1), \Lambda = \begin{pmatrix} -0.5 & 0.5 & 0 \\ 0.5 & -1 & 0.5 \\ 0 & 0.5 & -0.5 \end{pmatrix}$			
g, Σ_t	$\widehat{\mathcal{D}}(\hat{y}_t^{lim})$	$\widehat{\mathcal{D}}(\hat{y}_t^{del})$	$\widehat{\mathcal{D}}\left(\breve{y}_t^{\delta^{\frac{1}{2}}}\right)$ (note *)
$g = 0.01, \Sigma_t = 0.01$	0.4860	0.6432	0.0486
$\boldsymbol{g = 0.01, \Sigma_t = 0.03}$	**0.5491**	**0.6407**	*0.0729*
$\boldsymbol{g = 0.01, \Sigma_t = 0.1}$	**0.6107**	**0.6398**	0.1225
$g = 0.03, \Sigma_t = 0.03$	0.5660	0.6569	*0.0986*
$g = 0.1, \Sigma_t = 0.1$	0.6496	0.6796	0.1837
***Values coincide with Tab. 1**			
$\mathcal{E}\{\lvert y_\infty \rvert^2\} = \frac{2}{3} \approx 0.6667$			

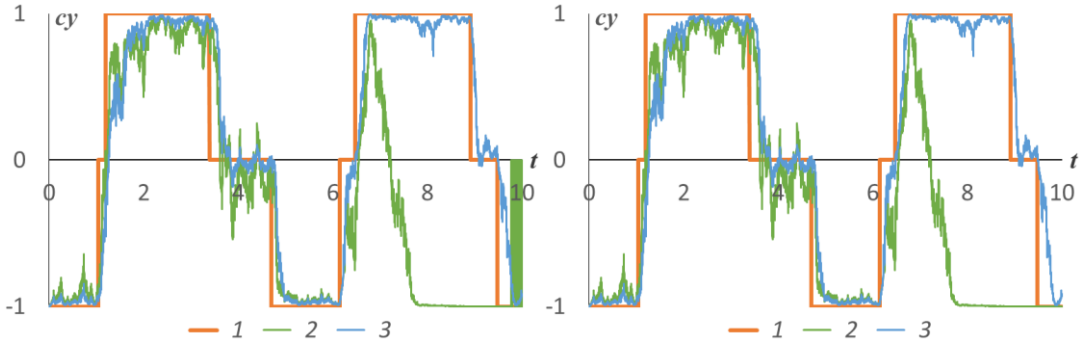

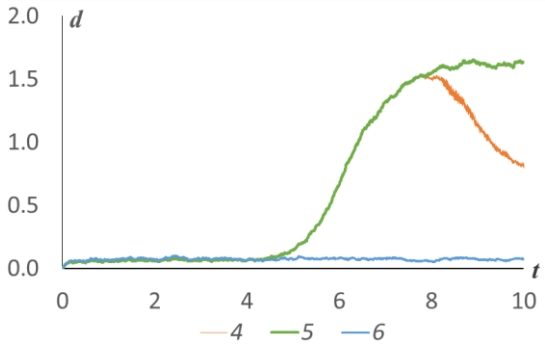

Fig. 6. Model 6, scenario 2: $g = 0.01, \Sigma_t = 0.03$

a,b) 1 – cy_t, 2 – $c\hat{y}_t^{lim}$ ($c\hat{y}_t^{del}$), 3 – $\breve{y}_{t_i}^{\delta^{\frac{1}{2}}}$

c) 4 – $\hat{d}_t(\hat{y}_t^{lim})$, 5 – $\hat{d}_t(\hat{y}_t^{del})$, 6 – $\hat{d}_t\left(\breve{y}_{t_i}^{\delta^{\frac{1}{2}}}\right)$

According to Tab. 6 the quality of the approximations $\hat{y}_t^{lim}$ and $\hat{y}_t^{del}$ should be claimed as inadmissible. It means that there is no robustness in the filters behavior. It can be stated as the main contribution of this series of experiments. In contrast to this the discretized filters preserve the robust properties. The evolution of the graph $\hat{d}_t(\hat{y}_t^{lim})$ deserves attention because its growth finalizes at some time moment and the accuracy of $\hat{y}_t^{lim}$ slightly improves. In fact, both algorithms stop estimating at some moment. It is visualized as sticking the green trajectory to line 1. It is also seen that the estimate $\hat{y}_t^{lim}$ begins to change while $\hat{y}_t^{del}$ does not.

By analogy with the stable case, current series of experiments are conducted for the models whose parameters coincide with the claimed ones in Tab. 1-5 except a, b. The results are given in Tab. 7-10 and complemented by graphs in Fig. 7-10.

Tab. 7. Experiment results. Unstable system.
The case of lager intensities

$a = 1, b = 0.5, n_y = 3, (c_1, c_2, c_3) = (-1, 0, 1), \Lambda = \begin{pmatrix} -5 & 5 & 0 \\ 5 & -1 & 5 \\ 0 & 5 & -5 \end{pmatrix}$			
g, Σ_t	$\widehat{\mathcal{D}}(\hat{y}_t^{lim})$	$\widehat{\mathcal{D}}(\hat{y}_t^{del})$	$\widehat{\mathcal{D}}\left(\breve{y}_t^{\delta^{\frac{1}{2}}}\right)$ (note *)
$g = 0.01, \Sigma_t = 0.01$	0.5674	0.7157	0.1948
$\boldsymbol{g = 0.01, \Sigma_t = 0.03}$	**0.6252**	**0.7097**	*0.2286*
$\boldsymbol{g = 0.01, \Sigma_t = 0.1}$	**0.7103**	**0.7348**	**0.3250**
$g = 0.03, \Sigma_t = 0.03$	0.6809	0.7643	*0.3064*
$g = 0.1, \Sigma_t = 0.1$	0.7880	0.8126	0.4485
***Values coincide with Tab. 2**			
$\mathcal{E}\{\lvert y_\infty \rvert^2\} = \frac{2}{3} \approx 0.6667$			

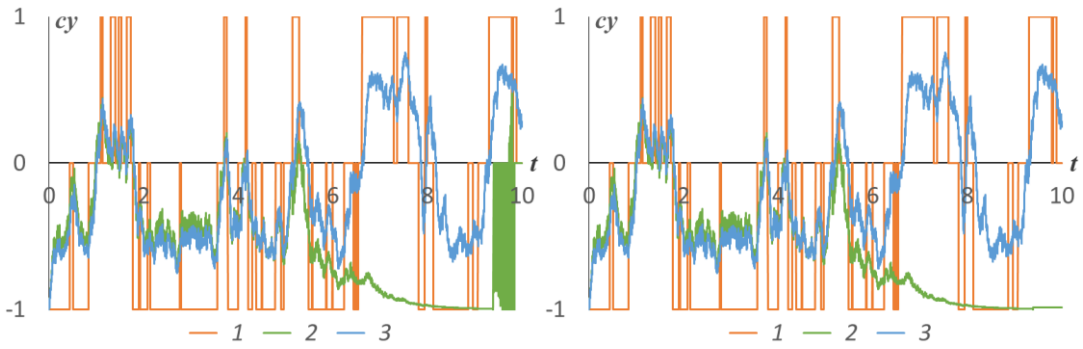

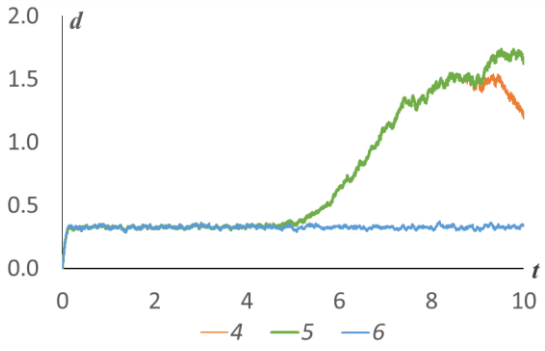

Fig. 7. Model 7, scenario 3: $g = 0.01, \Sigma_t = 0.1$

a,b) $1 - cy_t$, $2 - c\hat{y}_t^{lim}$ $(c\hat{y}_t^{del})$, $3 - \breve{y}_{t_i}^{\delta^{\frac{1}{2}}}$

c) $4 - \hat{d}_t(\hat{y}_t^{lim})$, $5 - \hat{d}_t(\hat{y}_t^{del})$, $6 - \hat{d}_t\left(\breve{y}_{t_i}^{\delta^{\frac{1}{2}}}\right)$

In the higher-dimensional state space the results reinforce conclusions made in the previous example. As it is clearly seen there is no robustness in the approximations evolutions.

Tab. 8. Experiment results. Unstable system.
The higher-dimensional state space case

$a = 1, b = 0.5, n_y = 4, c = (-1.5, -0.5, 0.5, 1.5), \Lambda = \begin{pmatrix} -0.5 & 0.5 & 0 & 0 \\ 0.5 & -1 & 0.5 & 0 \\ 0 & 0.5 & -1 & 0.5 \\ 0 & 0 & 0.5 & -0.5 \end{pmatrix}$			
g, Σ_t	$\widehat{\mathcal{D}}(\hat{y}_t^{lim})$	$\widehat{\mathcal{D}}(\hat{y}_t^{del})$	$\widehat{\mathcal{D}}\left(\breve{y}_t^{\delta^{\frac{1}{2}}}\right)$ (note *)
$g = 0.01, \Sigma_t = 0.01$	1.0222	1.3663	0.0534
$\boldsymbol{g = 0.01, \Sigma_t = 0.03}$	**1.1485**	**1.3604**	*0.0811*
$\boldsymbol{g = 0.01, \Sigma_t = 0.1}$	**1.2706**	**1.3450**	0.1384
$g = 0.03, \Sigma_t = 0.03$	1.1647	1.3711	*0.1086*
$g = 0.1, \Sigma_t = 0.1$	1.3076	1.3841	0.2058
***Values coincide with Tab. 3**			
$\mathcal{E}\{\|y_\infty\|^2\} = 1.25$			

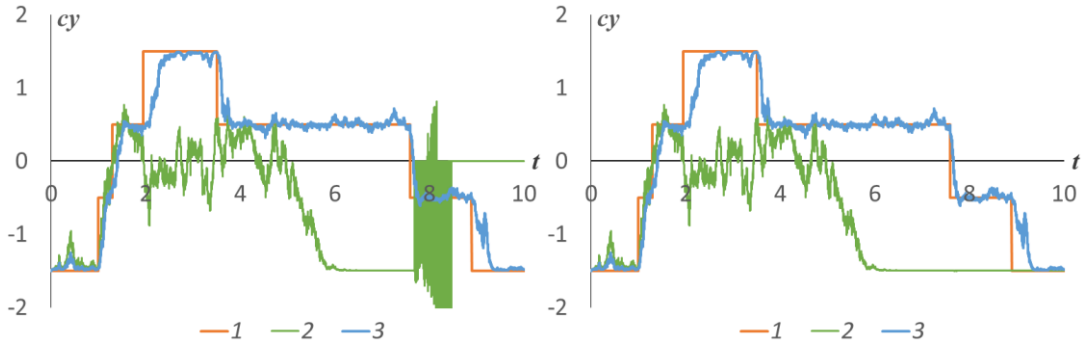

a) b)

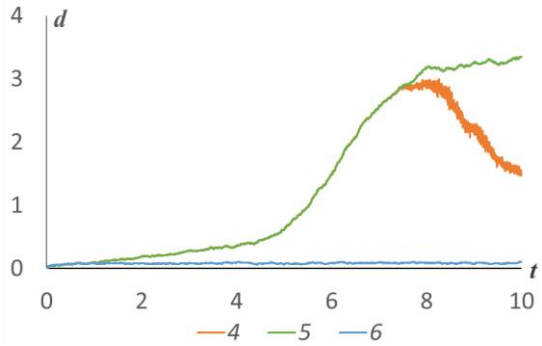

c)

Fig. 8. Model 8, scenario 2: $g = 0.01, \Sigma_t = 0.03$

a,b) 1 – cy_t, 2 – $c\hat{y}_t^{lim}$ ($c\hat{y}_t^{del}$), 3 – $\breve{y}_{t_i}^{\delta^{\frac{1}{2}}}$

c) 4 – $\hat{d}_t(\hat{y}_t^{lim})$, 5 – $\hat{d}_t(\hat{y}_t^{del})$, 6 – $\hat{d}_t\left(\breve{y}_{t_i}^{\delta^{\frac{1}{2}}}\right)$

Increasing intensity supports the inference made above.

Tab. 9. Experiment results. Unstable system.
The higher-dimensional state space case with larger intensities

$a = 1, b = 0.5, n_y = 4, c = (-1.5, -0.5, 0.5, 1.5), \Lambda = \begin{pmatrix} 5 & 5 & 0 & 0 \\ 5 & -1 & 5 & 0 \\ 0 & 5 & -1 & 5 \\ 0 & 0 & 5 & 5 \end{pmatrix}$

g, Σ_t	$\widehat{\mathcal{D}}(\hat{y}_t^{lim})$	$\widehat{\mathcal{D}}(\hat{y}_t^{del})$	$\widehat{\mathcal{D}}\left(\breve{y}_t^{\delta^{\frac{1}{2}}}\right)$ (note *)
$g = 0.01, \Sigma_t = 0.01$	1.3522	1.1722	0.2247
$\boldsymbol{g = 0.01, \Sigma_t = 0.03}$	**1.4753**	**1.6902**	*0.2665*
$\boldsymbol{g = 0.01, \Sigma_t = 0.1}$	**1.5672**	**1.6442**	0.3869
$g = 0.03, \Sigma_t = 0.03$	1.5516	1.76146	*0.3668*
$g = 0.1, \Sigma_t = 0.1$	1.7296	1.8053	0.5852
***Values coincide with Tab. 4** $\mathcal{E}\{\|y_\infty\|^2\} = 1.25$			

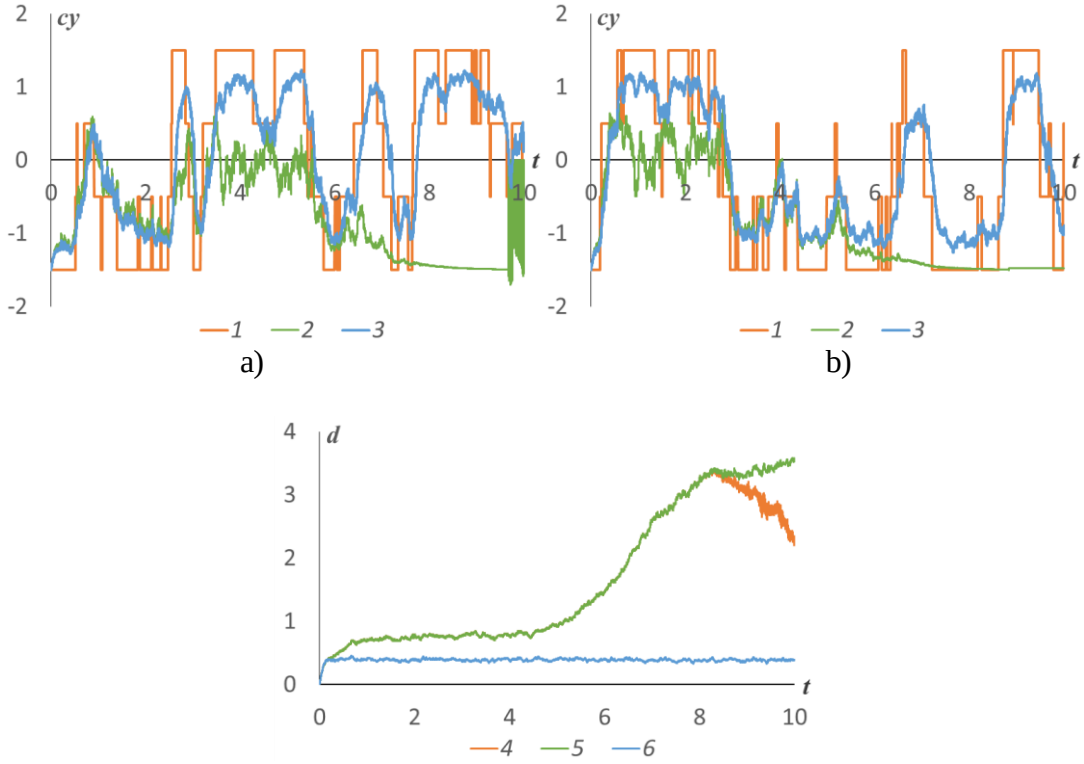

Fig. 9. Model 9, scenario 3: $g = 0.01, \Sigma_t = 0.1$

a,b) $1 - cy_t$, $2 - c\hat{y}_t^{lim}$ $(c\hat{y}_t^{del})$, $3 - \breve{y}_{t_i}^{\delta^{\frac{1}{2}}}$

c) $4 - \hat{d}_t(\hat{y}_t^{lim})$, $5 - \hat{d}_t(\hat{y}_t^{del})$, $6 - \hat{d}_t\left(\breve{y}_{t_i}^{\delta^{\frac{1}{2}}}\right)$

Besides the conclusions discussed above this experimental series brings out the fact that the estimates $\hat{y}_t^{lim}, \hat{y}_t^{del}$ lost their informativity conceding to the trivial estimate $\mathcal{E}\{y_t\}$ in accuracy.

Tab. 10. Experiment results. Unstable system.
The asymmetric case

$a = 1, b = 0.5, n_y = 3, c = (1,2,4), \Lambda = \begin{pmatrix} -0.5 & 0.5 & 0 \\ 0.5 & -1 & 0.5 \\ 0 & 0.5 & -0.5 \end{pmatrix}$			
g, Σ_t	$\widehat{\mathcal{D}}(\hat{y}_t^{lim})$	$\widehat{\mathcal{D}}(\hat{y}_t^{del})$	$\widehat{\mathcal{D}}\left(\breve{y}_t^{\delta^{\frac{1}{2}}}\right)$ (note *)
$g = 0.01, \Sigma_t = 0.01$	1.3522	1.1722	0.2247
$\boldsymbol{g = 0.01, \Sigma_t = 0.03}$	**1.4753**	**1.6902**	*0.2665*
$\boldsymbol{g = 0.01, \Sigma_t = 0.1}$	**1.5672**	**1.6442**	0.3869
$g = 0.03, \Sigma_t = 0.03$	1.5516	1.76146	*0.3668*

$g = 0.1, \Sigma_t = 0.1$	1.7296	1.8053	0.5852

***Values coincide with Tab. 5**

$$\mathcal{E}\{|y_\infty - \mathcal{E}\{y_\infty\}|^2\} = \frac{14}{9} \approx 1{,}5556$$

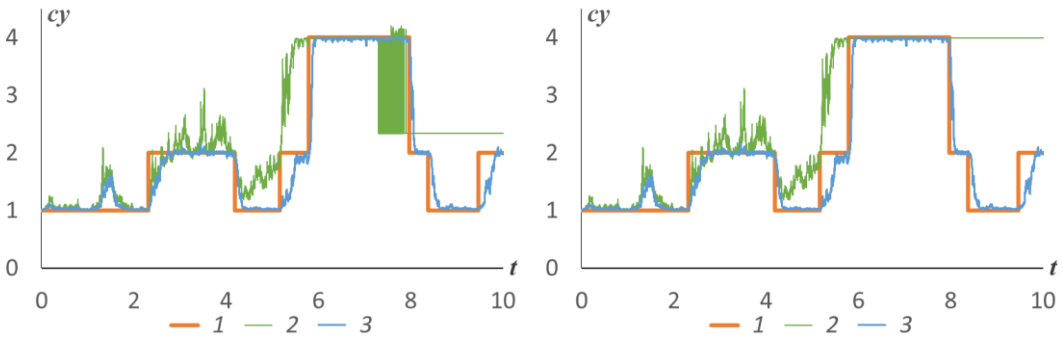

a) b)

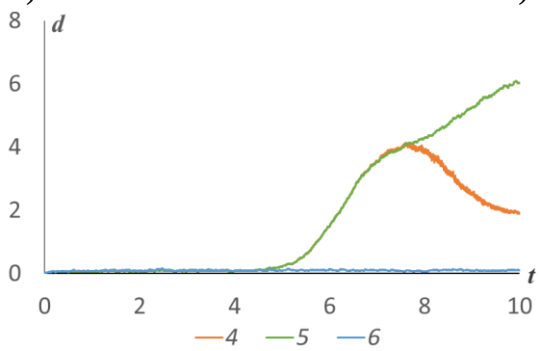

c)

Fig. 10. Model 10, scenario 2: $g = 0.01, \Sigma_t = 0.03$

a,b) $1 - cy_t$, $2 - c\hat{y}_t^{lim}$ $(c\hat{y}_t^{del})$, $3 - \breve{y}_{t_i}^{\delta^{\frac{1}{2}}}$

c) $4 - \hat{d}_t(\hat{y}_t^{lim})$, $5 - \hat{d}_t(\hat{y}_t^{del})$, $6 - \hat{d}_t\left(\breve{y}_{t_i}^{\delta^{\frac{1}{2}}}\right)$

Thus, the last results demonstrate identical behavior of the approximations $\hat{y}_t^{lim}, \hat{y}_t^{del}$ with poor accuracy of the estimates close to or even worse than the trivial estimate $\mathcal{E}\{y_t\}$. In contrast, estimates based on the discretized filters don't depend on whether the measurement system is stable or not. That agrees with theory. In all the cases the discretized filters preserve the robust properties with respect to uncertainty whereas the approximations of the Wonham filter cannot demonstrate these properties.

5. Conclusion

The paper discusses and proposes approaches to forming stable numerical implementations of the Wonham filter with uncertainty in measurement noise covariance. The exact filtering problem is tough to obtain. However, if supposing that there is no uncertainty in the model the optimal solution is provided by the Wonham filter. Unfortunately, such an approach cannot be considered as the way out because the numerical implementations of the Wonham filter suffer from divergence. Consequently, effective numerical implementations that additionally show robustness are of interest. Because of lack of analytical solutions the examination of the filters behavior are conducted with a wide range of series of numerical experiments. The obtained results showcase that all the filters (the discretized filters, the Wonham filter approximations) preserve the robust properties with respect to uncertainty in the stable measurements case. Absolutely opposite behavior can be observed when switching to unstable measurements. The discretized filters take advantages in estimation in comparison with the approximations. With a certain set of the parameters of the model, it is found that approximations even becomes out of sense, and do not preserve the robust property

at all as a result. Thus, benefits of the discretized filters are absolutely undoubtedly in the problem under uncertainty in the unstable measurements case.

References

[1] Kalman R.E., Bucy R.S. New results in linear filtering and prediction theory. *Trans. ASME J. Basic Eng.*, **83**(1), 95–108 (1961)

[2] Anderson B.D.O., Moore J.B. *Optimal filtering*. Prentice Hall (1989)

[3] Davis M.H.A., Marcus S.I. An Introduction to Nonlinear Filtering. *Stochastic Systems: The Mathematics of Filtering and Identification and Applications. NATO Advanced Study Institutes Series*, **78**, 53–75 (1980)

[4] Beneš V.E. Exact finite-dimensional filters for certain diffusions with nonlinear drift. *Stochastics*, **5**, 65–92 (1981)

[5] Daum F.E. Exact finite-dimensional nonlinear filters. *IEEE Trans. Autom. Control*, **31**, 616–622 (1986)

[6] Yaz E. Linear state estimators for non-linear stochastic systems with noisy non-linear observations. *Int. J. Control*, **48**, 2465–2475 (1988)

[7] Bernstein D.S., Haddad W.M. Steady-state Kalman filtering with an H∞ error bounded. *Syst. Control. Lett.*, **12**, 9–16 (1989)

[8] Li H., Shi Y. Robust H∞ filtering for nonlinear stochastic systems with uncertainties and Markov delays. *Automatica*, **48**, 159–166 (2012)

[9] Geromel J.C., Bernussou J., Garcia. G., Oliveira M.C.D. H2 and H∞ robust filtering for discrete-time linear systems. *SIAM J. Control Optim.*, **38**, 1353–1368 (2000)

[10] Rao C.V., Rawlings J.B., Mayne D.Q. Constrained state estimation for nonlinear discrete-time systems: stability and moving horizon approximations. *IEEE Trans. Autom. Control*, **48**, 246–258 (2003)

[11] Alessandri A., Baglietto M., Battistelli G. A minimax receding-horizon estimator for uncertain discrete-time linear systems. In Proceedings of the 2004 American Control Conference, Boston, MA, USA, 30 June – 2 July 2004, 205–210.

[12] Geromel J.C. Optimal linear filtering under parameter uncertainty. *IEEE Trans. Signal Process*, **47**, 168–175 (1999)

[13] Verdu S., Poor H. Minimax linear observers and regulators for stochastic systems with uncertain second-order statistics. *IEEE Trans. Autom. Contr.*, **29**, 499–511 (1984)

[14] Verdu S., Poor H. On minimax robustness: a general approach and applications. *IEEE Trans. Inf. Theory*, **30**, 328–340 (1984)

[15] Poor V., Looze D. Minimax state estimation for linear stochastic systems with noise uncertainty. *IEEE Trans. Autom. Control*, **26**, 902–906 (1981)

[16] Miller G.B., Pankov A.R. Minimax filtering in linear stochastic uncertain discrete-continuous systems. *Autom. Remote Control*, **67**, 413–427 (2006)

[17] Miller G.B., Pankov A.R. Minimax control of a process in a linear uncertain-stochastic system with incomplete data. *Autom. Remote Control*, **68**, 2042–2055 (2007)

[18] Wonham W.M. Some applications of stochastic differential equations to optimal nonlinear filtering. *SIAM J. Control*, **2**, 347–369 (1965)

[19] Elliott R.J., Aggoun L., Moore J.B. *Hidden Markov Models: Estimation and Control*. Springer (1995)

[20] Kloeden P.E., Platen E. *Numerical Solution of Stochastic Differential Equations*. Springer (1992)

[21] Yin G., Zhang Q., Liu, Y. Discrete-time approximation of Wonham filters. *J. Control Theory Appl.*, **2**, 1–10 (2004)

[22] Borisov A.V. L1-optimal filtering of Markov jump processes. II. Numerical analysis of particular realizations schemes. *Autom. Remote Control*, **81**, 2160–2180 (2020)

[23] Borisov A.V., Bosov A.V. Practical implementation of the solution of the stabilization problem for a linear system with discontinuous random drift by indirect observations. *Autom. Remote Control*, **83**, 1417–1432 (2022)
[24] Vandelinde V. Robust properties of solutions to linear-quadratic estimation and control problems. *IEEE Trans. Autom. Control*, **22**, 138–139 (1977)
[25] Morris, J. The Kalman filter: A robust estimator for some classes of linear quadratic problems. *IEEE Trans. Inf. Theory*, **22**, 526–534 (1976)